PHYSICAL REVIEW D **88,** 016008 (2013)

Revisiting the phase diagram of the three-flavor quark system in the Nambu–Jona-Lasinio model

Li-jia Jiang (姜丽佳), Xian-yin Xin (辛现银), Kun-lun Wang (王昆仑), and Si-xue Qin (秦思学)*
Department of Physics and State Key Laboratory of Nuclear Physics and Technology, Peking University, Beijing 100871, China

Yu-xin Liu (刘玉鑫)†
Department of Physics and State Key Laboratory of Nuclear Physics and Technology, Peking University, Beijing 100871, China and Center for High Energy Physics, Peking University, Beijing 100871, China
(Received 22 March 2013; published 19 July 2013)

We propose the 2 + 1 flavor chiral susceptibility criterion to identify the chiral phase transition of the 2 + 1 flavor quark system and take it to determine the phase boundary and the critical end point (CEP) in the Nambu-Jona-Lasinio model. We give explicitly the phase diagram of the 2 + 1 flavor quark system in terms of the temperature, quark chemical potential and strange quark mass and that in terms of the temperature, quark chemical potential, and flavor-mixing interaction strength. We locate the CEP of the 2 + 1 quark system with physical masses at $(\mu_E, T_E) = (316.2\ \text{MeV}, 68.1\ \text{MeV})$. We show that increasing the mass of the strange quark lowers the temperature and enhances the chemical potential of the CEP if the mass is not quite large, and there exists a critical flavor-mixing interaction strength $(K\Lambda^5)_c \approx 6.05$ for the crossover to turn into a first order phase transition. Increasing the flavor-mixing strength beyond the critical one induces the temperature of the CEP to increase drastically and raises slightly at first and then descends the chemical potential.

DOI: 10.1103/PhysRevD.88.016008 PACS numbers: 11.30.Rd, 11.10.Wx, 12.38.Aw, 21.65.Qr

I. INTRODUCTION

The properties of strong interaction matter at finite temperature and baryon density have gotten both theoretical and experimental attention for decades [1–9], while determining the QCD phase diagram is one of the main subjects [7–9], since an exact depiction of the phase diagram will provide fundamental understanding of the origin of mass, the mechanism of color confinement (hadronization), and the evolution of early universe matter. However, the phase diagram of QCD is proved to be complicated, because it is governed by not only the medium effects of temperature, density (or chemical potential), and finite size, but also the intrinsic effects of current quark mass, isospin, interaction strength, color-flavor structure, and so forth. Intensive searches on high energy heavy-ion collisions have been performed at laboratories such as the RHIC and LHC, and a promising observation of signatures of the phase diagram is being looked forward to. Observation of the properties of compact stars provides a natural laboratory for exploring the properties of very dense strong interaction matter. At the same time, kinds of quantum field theory approaches and phenomenological models have been developed to try to get close to the essence of the phase transitions, mainly the chiral phase transition and deconfinement-confinement phase transition. Lattice gauge theory is quite successful in the nonperturbative region of QCD [10–12], except the so-called fermion sign problem which obstructs its application on nonzero chemical potential circumstance. Efforts have been made to overcome such a problem and great progress has been made (see, for example, Refs. [13–23]). On the continuous field theory side, besides that the Dyson-Schwinger equation approach [24–28] has been applied to explore the QCD phase transitions (see, for instance, Refs. [29–40]), the Nambu-Jona-Lasinio (NJL) model [41,42], the chiral quark model [43,44], the quark meson coupling (QM) model [45], and other effective models and their improvement to taking into account the confinement effect (for instance, Polyakov-loop improved NJL (PNJL) model, Polyakov-loop improved QM model, etc.) [46–52] have also been implemented to study the QCD phase transitions. Then not only the general features of the phase diagram but also the critical end point (CEP) of the transitions have been proposed (see for example, Refs. [13–18,33,34,37,38,47–49,53–69]). Especially, the variation behaviors of the phase boundaries and the CEP's location with respect to the interaction strength, the flavor-mixing strength, the u- (and d-)quark mass, and the strange quark mass have been given in some sense (see, for instance, Refs. [17,37,47,49,55,56,59,61,64,69]) Moreover, with the interactions being extended to include the diquark related channels, in particular, the six-point diquark chiral coupling which is a type of $U_A(1)$ anomaly, a new critical point and some other interesting phenomena are proposed [70–73]. However, whether the QCD critical end point really exists or not is still an open question

*Present address: Institute for Theoretical Physics, Johann Wolfgang Goethe University, D-60438 Frankfurt am Main, Germany.
†Corresponding author.
yxliu@pku.edu.cn

(see, for instance, Refs. [74,75]). We revisit then the phase diagram of the 2 + 1 flavor quark system in the NJL model with a newly proposed criterion to determine the phase boundary and the CEP in this paper.

In this paper, we investigate the chiral phase transition of the 2 + 1 flavor quark system in the NJL model by extending the recently proposed chiral susceptibility criterion to determine the phase boundary and the location of the CEP for a one-flavor (or two symmetric flavor) quark system [35,37,76] to a three-flavor one. With the new criterion, we give the phase diagram of the 2 + 1 flavor quark system in terms of the temperature, quark chemical potential, and strange quark mass and that in terms of the temperature, quark chemical potential and flavor-mixing interaction strength. We locate the CEP of the 2 + 1 flavor quark system with physical masses and discuss the current quark mass and the flavor-mixing six-point interaction [another type of $U_A(1)$ anomaly] effects on the phase diagram and, especially the location of the CEP.

The paper is organized as follows. In Sec. II, we describe briefly the NJL model of the 2 + 1 flavor quark system at finite temperature and finite quark chemical potential and extend the chiral susceptibility criterion for a one-flavor system to a three-flavor system. In Sec. III, we present the numerical results and discuss the chiral phase transition of the 2 + 1 flavor quark system and the effects of the strange quark mass and the flavor-mixing interaction strength on the phase boundary and the CEP. In Sec. IV, we give a brief summary and remark.

II. THE MODEL

The Lagrangian of the three-flavor NJL model at finite chemical potential is written as

$$\begin{aligned}\mathcal{L}_{\mathrm{NJL}} &= \bar{\psi}(i\gamma\cdot\partial + \gamma_0\hat{\mu} - \hat{m})\psi \\ &\quad + G\sum_{i=0}^{8}[(\bar{\psi}\tau_i\psi)^2 + (\bar{\psi}i\gamma_5\tau_i\psi)^2] \\ &\quad - K[\det{}_f(\bar{\psi}(1+\gamma_5)\psi) + \det{}_f(\bar{\psi}(1-\gamma_5)\psi)],\end{aligned} \tag{1}$$

where $\psi = \{u, d, s\}$ is the three-flavor quark field; $\hat{\mu} = \mathrm{diag}\{\mu_u, \mu_d, \mu_s\}$ is the chemical potential matrix; $\hat{m} = \mathrm{diag}\{m_u, m_d, m_s\}$ is the current quark mass matrix; $\tau_0 = \sqrt{2/3}\mathbf{I}_{3\times3}$, while $\tau_{i\neq0}$ are the eight Gell-Mann matrices in flavor $SU(3)$ space; and G and K are the coupling constants of four-point and six-point interaction (flavor-mixing) strength separately. Note that the t'Hooft six-point interaction (i.e., the triple chiral coupling) breaks the $U_A(1)$ symmetry, it is then referred to as a type of $U_A(1)$ anomaly. Usually, $m_u = m_d \neq m_s$ is taken, which breaks the $SU_f(3)$ symmetry explicitly, but reserves the isospin symmetry at the Lagrangian level. In principle, the chemical potential of each flavor can then differ from each other, i.e., $\mu_u \neq \mu_d \neq \mu_s$. For simplicity, an identical chemical potential for the three flavors is set herein.

Treating the field with chiral quark condensate as a global mean field, we have the thermodynamical potential of the system,

$$\begin{aligned}\Omega &= 2G(\phi_u^2 + \phi_d^2 + \phi_s^2) - 4K\phi_u\phi_d\phi_s \\ &\quad - 2N_cT\sum_{i=u,d,s}\int\frac{d^3\vec{p}}{(2\pi)^3}[\theta(\Lambda^2 - \vec{p}^2)\beta E_i \\ &\quad + \ln(1 + e^{-\beta(E_i+\mu)}) + \ln(1 + e^{-\beta(E_i-\mu)})],\end{aligned} \tag{2}$$

where the coefficient 2 is the spin degrees of freedom, $N_c = 3$ is the number of colors, μ is the chemical potential, T is the temperature and $\beta = 1/T$, $\phi_i = \langle\bar{\psi}\psi\rangle_i$ $(i = u, d, s)$ is the chiral condensate of quarks with flavor i, and E_i $(i = u, d, s)$ is the quasiparticle energy, which reads $E_i = \sqrt{\vec{p}^2 + M_i^2}$, with the constituent quark mass of flavor i expressed as

$$M_i = m_i - 4G\phi_i + 2K\phi_j\phi_k, \qquad (i \neq j \neq k). \tag{3}$$

Since the NJL model is nonrenormalizable, an ultraviolet cutoff is introduced to eliminate the divergence of the integral. In practical calculations, the parameter set established in Ref. [77] is commonly adopted: $m_u = m_d = 5.5$ MeV, $m_s = 140.7$ MeV, $\Lambda = 602.3$ MeV, $G\Lambda^2 = 1.835$, and $K\Lambda^5 = 12.36$, which are fixed by fitting $m_\pi = 135.0$ MeV, $m_K = 497.7$ MeV, $m_{\eta'} = 957.8$ MeV, $f_\pi = 92.4$ MeV, and $\phi_{u,d,0} = \langle\bar{q}q\rangle_{u,d,0} = -(242\ \mathrm{MeV})^3$. The equations of motion can be obtained from minimizing the thermodynamical potential in Eq. (2) with respect to ϕ_u, ϕ_d, and ϕ_s,

$$\frac{\partial\Omega}{\partial\phi_u} = \frac{\partial\Omega}{\partial\phi_d} = \frac{\partial\Omega}{\partial\phi_s} = 0. \tag{4}$$

As the same current mass is taken to u and d quarks, they behave in the same way, thus light quark is adopted to represent both u- and d-quark hereafter. This set of equations can be solved as functions of temperature T and chemical potential μ. One can then obtain the property of the stable phase by analyzing the configurations of the fields corresponding to the minimum (or minima) of the thermodynamical potential. Furthermore, one can identify a phase transition as the global minimum of the Ω shifts from one to another. More directly, one usually takes the derivative of the chiral quark condensate with respect to the temperature or chemical potential,

$$\chi_T = -\frac{\partial\phi}{\partial T}, \qquad \chi_\mu = -\frac{\partial\phi}{\partial\mu}, \tag{5}$$

to identify a phase transition.

Current lattice QCD simulations have provided a strong implication that the phase transition of chiral symmetry at vanishing chemical potential is a continuous, nonsingular but rapid crossover [10,19] when physical masses are

taken. Because of the nonsingularity of the crossover, the value of pseudocritical temperature (T_c) is different, depending on the choice of the signatures (observables) identifying the phase evolution. However, when it comes to first order phase transition, the choice does not influence the value of the transition temperature and chemical potential. In another point of view, if the thermodynamical potential is available, the sign of the second order derivative of the potential with respect to the order parameter(s) is an excellent measure identifying the stability of the phase. More explicitly, the phase changes from stable to unstable if the sign shifts from positive to negative. In the Nambu-Jona-Lasinio model, it has been shown that the sign of the second order derivative of the potential is exactly the same as that of the chiral susceptibility [76],

$$\chi_c = \frac{\partial M}{\partial m_0}\bigg|_{m_0=0}, \tag{6}$$

where M is the constituent quark mass which identifies the chiral symmetry breaking and m_0 is the current quark mass. Or equivalently,

$$\chi_c = -\frac{\partial\langle\bar{q}q\rangle}{\partial m_0}\bigg|_{m_0=0}, \tag{7}$$

where $\langle\bar{q}q\rangle = \phi$ is the chiral quark condensate. Because of the nonperturbative nature, it is impossible for us to have explicitly the thermodynamical potential when taking the sophisticated nonperturbative approaches of QCD. The traditional criterion of analyzing the effective thermodynamical potential should then be replaced by other ones. Considering the above-mentioned equivalence of the sign of the second order derivative of the thermodynamical potential and that of the chiral susceptibility, one can naturally take the chiral susceptibility as a criterion. Practical calculations for a one-flavor quark system indicate that the criterion of chiral susceptibility works still well in the chiral limit when one takes the nonperturbative nature, such as with sophisticated models for the Dyson-Schwinger equations of QCD [37]. We then, in this paper, extend the one-flavor chiral susceptibility to a three-flavor chiral susceptibility and take it to locate the transition point for both crossover and first order phase transition. Along the line of the one-flavor chiral susceptibility, the chiral susceptibility of the three-flavor quark system is defined as

$$\chi_{ij} = -\frac{\partial\phi_i}{\partial m_j}, \tag{8}$$

which is a 3×3 matrix (with $i = u, d, s$). Because of the flavor-mixing interaction, the off-diagonal elements are nonvanishing. After some calculations, one can obtain the relation of the second order derivative of the thermodynamical potential $\frac{\partial^2\Omega}{\partial\phi_i\phi_j}$ and the chiral susceptibility χ_{ij} as

$$\begin{pmatrix} \frac{\partial^2\Omega}{\partial\phi_u^2} & \frac{\partial^2\Omega}{\partial\phi_d\phi_u} & \frac{\partial^2\Omega}{\partial\phi_s\phi_u} \\ \frac{\partial^2\Omega}{\partial\phi_u\phi_d} & \frac{\partial^2\Omega}{\partial\phi_d^2} & \frac{\partial^2\Omega}{\partial\phi_s\phi_d} \\ \frac{\partial^2\Omega}{\partial\phi_u\phi_s} & \frac{\partial^2\Omega}{\partial\phi_d\phi_s} & \frac{\partial^2\Omega}{\partial\phi_s^2} \end{pmatrix}\begin{pmatrix} \chi_{uu} & \chi_{ud} & \chi_{us} \\ \chi_{du} & \chi_{dd} & \chi_{ds} \\ \chi_{su} & \chi_{sd} & \chi_{ss} \end{pmatrix}$$
$$= -\begin{pmatrix} C(M_u)(-4G) & C(M_u)(2K\phi_s) & C(M_u)(2K\phi_d) \\ C(M_d)(2K\phi_s) & C(M_d)(-4G) & C(M_d)(2K\phi_u) \\ C(M_s)(2K\phi_d) & C(M_s)(2K\phi_u) & C(M_s)(-4G) \end{pmatrix}, \tag{9}$$

where $C(M_i)$ is a function of constituent quark mass M_i which has the form

$$C(M_i) = 2\int\frac{d^3\vec{p}}{(2\pi)^3}\left\{A(E_i)\frac{\vec{p}^2}{E_i^3} + B(E_i)\left(\frac{M_i}{E_i}\right)^2\right\}, \tag{10}$$

with

$$A(E_i) = -\frac{3e^{-(E_i-\mu)/T}}{1+e^{-(E_i-\mu)/T}} - \frac{3e^{-(E_i+\mu)/T}}{1+e^{-(E_i+\mu)/T}} + 3\theta(\Lambda^2-\vec{p}^2),$$
$$B(E_i) = \frac{3}{T}\frac{e^{-(E_i-\mu)/T}}{1+e^{-(E_i-\mu)/T}} - \frac{3}{T}\left(\frac{e^{-(E_i-\mu)/T}}{1+e^{-(E_i-\mu)/T}}\right)^2 + \frac{3}{T}\frac{e^{-(E_i+\mu)/T}}{1+e^{-(E_i+\mu)/T}} - \frac{3}{T}\left(\frac{e^{-(E_i+\mu)/T}}{1+e^{-(E_i+\mu)/T}}\right)^2.$$

It is apparent that $B(E_i)$ is positive definite. We have carefully checked that $A(E_i)$ is also positive in the relevant region we are interested in. Meanwhile the diagonal element $(-4G)$ always has a higher magnitude than the off-diagonal elements $2K\phi_i$. Then, the determinant of the matrix in the right-hand side of Eq. (9) would be negative definite. Labeling the matrix in the right-hand side as $\mathcal{M}$, and taking the determinant on both sides of Eq. (9), we can express the relation simply as

$$\det(\chi_{ij}) = -\frac{\det\mathcal{M}}{\det(\frac{\partial^2\Omega}{\partial\phi_j\phi_i})}. \tag{11}$$

It is evident that the sign of $\det(\chi)$ is in accord with the sign of $\det(\frac{\partial^2\Omega}{\partial\phi_j\phi_i})$ in the region with which we are concerned.

As mentioned above, the concavo-convexity of thermodynamical potential is determined by the second order derivative of itself, one can then identify the stability of a phase by the sign of the second order derivative. As a consequence, one can take the shift of the sign of the chiral susceptibility as a signature of the phase transition of the one-flavor quark system [35,37,76]. In the case of the three-flavor NJL model, it is a little more complicated. We have to judge the positive definiteness of the upper matrix. For a concavo or convexity case, a mere determinant of the matrix is enough for us, as the rank of the matrix is odd, and the determinant is positive or negative,

respectively. However, for a saddle type, it can give rise to both a positive or a negative situation depending on the number of negative eigenvalues, thus each sign of the eigenvalues have to be checked exactly. To be more effective, we redefine the chiral susceptibility by multiplying the absolute value of Eq. (11) by a sign factor as

$$\chi' = \hat{\lambda}_0 |\det(\chi)|, \tag{12}$$

where $\hat{\lambda}_0$ stands for the sign of matrix χ's minimal eigenvalue and carries a dimension of GeV^{-6} to make χ' dimensionless. Although this expression is not complete to distinguish whether a unstable state is at a saddle point or at a local maximum, it is enough for us to identify a stable state. The numerical results of chiral susceptibilities we show in the next section are just that in such an expression and are rewritten as χ for simplicity.

With the above and previous results in mind, we know that the chiral susceptibilities of the two phases diverge or hump at the same point (state) if the evolution between them is a second order phase transition or a crossover (if the Wigner solution corresponding to the chiral symmetric phase exists) but at different locations for a first-order phase transition typically. Then the point which separates the regions in which the chiral susceptibilities of the two phases diverge at different states or at the same state is just the CEP. It follows that simultaneous analysis of the chiral susceptibilities of the two phases can chart the phase diagram, and hence establish the existence and location of the CEP.

III. NUMERICAL RESULTS AND DISCUSSION

A. In the chiral limit

As a starting point, we discuss the case in the chiral limit, in which the current masses of the three kinds of quarks are set to be zero, i.e., $m_u = m_d = m_s = 0$, while other variables ϕ_i $(i = u, d, s)$ are distinguishable.

The calculated results (with the interaction strength and the cutoff parameters established in Ref. [77] and listed explicitly in last section) of the temperature dependence of the relative chiral quark condensates (or normalized quark condensates) $\phi_i/\phi_{i,0}$ at zero chemical potential, $\mu = 0$, are shown in Fig. 1. It is evident that there exists always a zero definite solution, which is just the conventionally denoted "Wigner" solution, corresponding to the chiral symmetry phase. Besides, there exist nonzero solutions at low temperature, which are the conventionally denoted "Nambu" solutions, corresponding to the chiral symmetry broken phase. Different from the one-flavor case, the positive-negative symmetry of the Nambu phase(s) is violated due to the flavor-mixing interaction (the term $4K\phi_u\phi_d\phi_s$ in thermodynamical potential). In addition, there exists a region of temperature for multisolutions. To be more explicit, we refer to them as "Nambu +," "Nambu −," "Nambu Int" (a part of the multisolutions shown in red in the figure, i.e., the intermediate part), respectively.

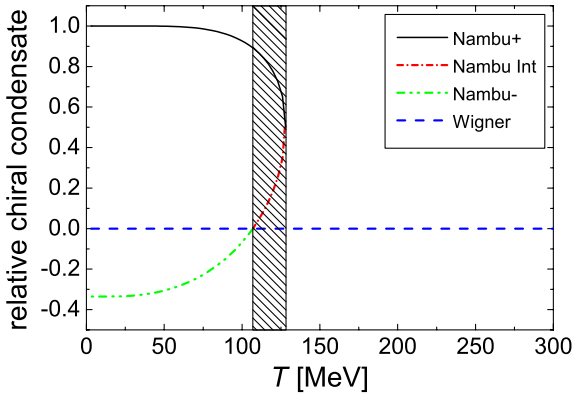

FIG. 1 (color online). Calculated temperature dependence of the relative chiral quark condensate in the chiral limit at zero chemical potential.

In Fig. 2, we display the calculated temperature dependence of the thermodynamical potential density $\Omega(T) = \Omega[\phi_u(T), \phi_d(T), \phi_s(T); T; \mu = 0]$. It is apparent that, at low temperature, the $\Omega(T)$ of the Nambu+ phase, Nambu −, Wigner phase, is the global minimum, local minimum (in fact a saddle point when considering other effects), global maximum, respectively, while, at high temperature, the $\Omega(T)$ of the Wigner phase is the global minimum (in fact, the unique minimum). More detailed data show that the Nambu− phase coalesces with the Nambu intermediate at temperature $T = 107.1$ MeV, and the $\Omega(T)$ of the Wigner phase becomes the local minimum simultaneously. As the temperature goes up, that of the Nambu+ phase maintains the global minimum to $T = 125.8$ MeV, at which the Nambu+ phase and the Wigner phase have the equivalent thermodynamical potential (displayed in the inset). As the temperature increases further, the $\Omega(T)$ of the Wigner phase is always the global

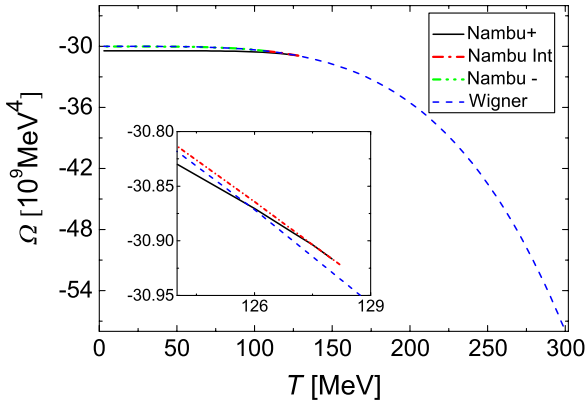

FIG. 2 (color online). Calculated temperature dependence of the thermodynamical potential in the chiral limit at zero chemical potential.

minimum, and those of the Nambu+ phase and Nambu intermediate phase vanish at $T = 128.2$ MeV. It manifests that there exists a temperature driven first order phase transition from the chiral symmetry broken to the chiral symmetric, $T \in (107.1, 128.2)$ MeV is the coexisting region. In Fig. 3, we show the variation behaviors of the chiral susceptibilities corresponding to the three solutions. It is quite easy to recognize from the figure that the chiral susceptibility of the Nambu+ phase is always positive before it diverges at temperature $T = 128.2$ MeV, the susceptibilities corresponding to the Nambu− and Nambu intermediate solutions are negative definite even though there involves a divergent point at $T = 107.1$ MeV, while the susceptibility of the Wigner solution diverges at $T = 107.1$ MeV and changes from negative to positive. Such a variation feature of the chiral susceptibility indicates also a temperature driven first order phase transition from the chiral symmetry broken to the chiral symmetric. It is remarkable that such a temperature driven phase evolution characteristic of a three-flavor quark system in the chiral limit is completely different from that in the one-flavor case where it is in second order or crossover (see, for example, Refs. [6,53]).

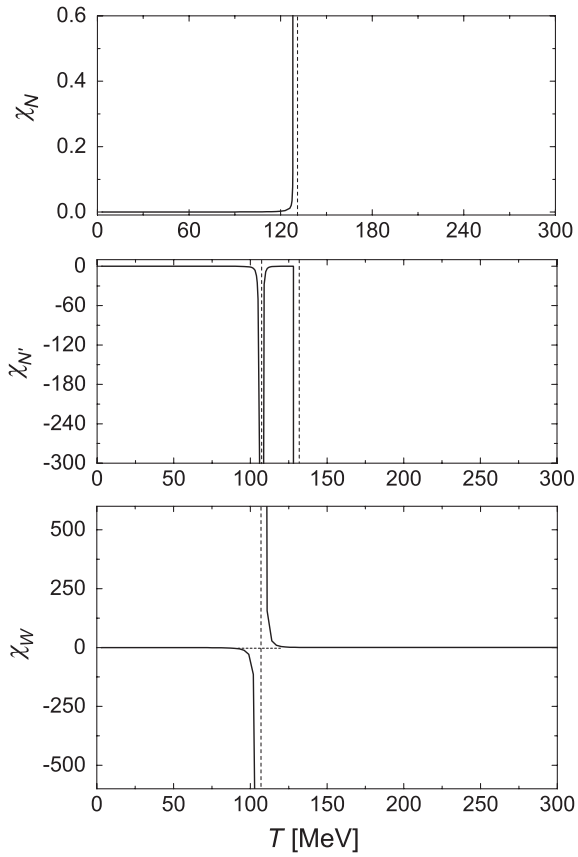

FIG. 3. Calculated temperature dependence of the chiral susceptibilities at zero chemical potential: upper panel for Nambu+ phase; middle panel for Nambu intermediate and Nambu− state; lower panel for Wigner phase.

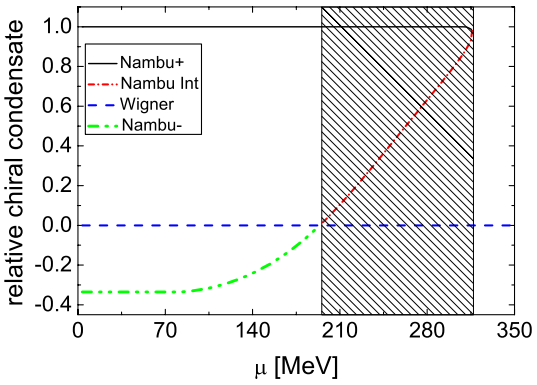

FIG. 4 (color online). Calculated chemical potential dependence of the relative chiral quark condensate of the three-flavor quark system in the chiral limit at zero temperature.

Next, we discuss the case of the three-flavor quark system in the chiral limit at finite chemical potential but zero temperature. The calculated variation behavior of the relative chiral quark condensate with respect to the chemical potential is shown in Fig. 4, while the corresponding thermodynamical potential density and chiral susceptibility are displayed in Figs. 5 and 6, respectively. It is apparent that the variation behaviors of the three quantities are qualitatively the same as that of the corresponding one at finite temperature and zero chemical potential. We can reach then that increasing the quark chemical potential also drives a first order phase transition from the chiral symmetry broken to the chiral symmetric for the three-flavor quark system in the chiral limit, which is the same as that for the one-flavor case. Moreover, the phase coexistence region is $\mu \in (195.4, 320.4)$ MeV, and the traditional way of analyzing the thermodynamical potential gives the critical chemical potential $\mu_c = 281.8$ MeV.

To discuss the phase evolution behavior of the system at both finite temperature and finite chemical potential, we present the temperature dependence of the relative chiral

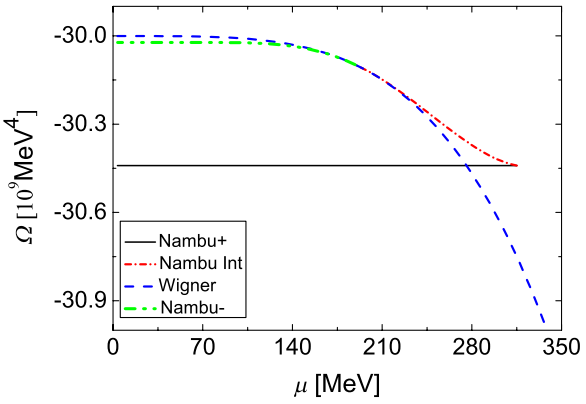

FIG. 5 (color online). Calculated chemical potential dependence of the thermodynamical potential of the three-flavor quark system in the chiral limit at zero temperature.

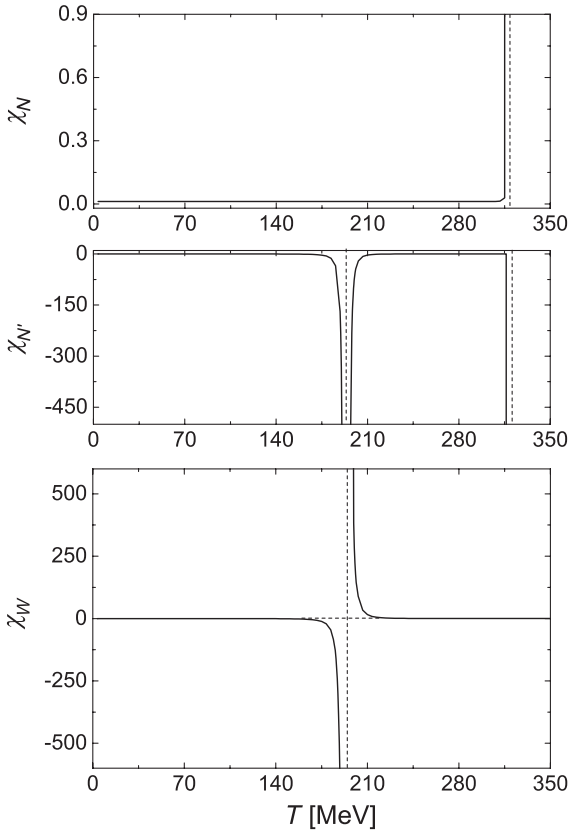

FIG. 6. Calculated chemical potential dependence of the chiral susceptibility of the three-flavor quark system in the chiral limit at zero temperature: upper panel, the Nambu+ phase; middle panel, the Nambu− and Nambu intermediate state; lower panel, the Wigner phase.

quark condensates at several values of chemical potential in Fig. 7 and those of the chiral susceptibilities of Nambu and Wigner solutions in Fig. 8. It is obvious that the Wigner phase whose chiral quark condensate is always zero exists at all the values of chemical potential, and the Nambu− phase with negative relative chiral condensate exists only

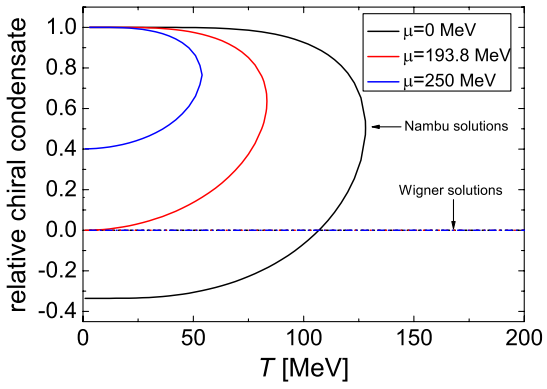

FIG. 7 (color online). Calculated temperature dependence of the relative chiral quark condensate at several values of chemical potential.

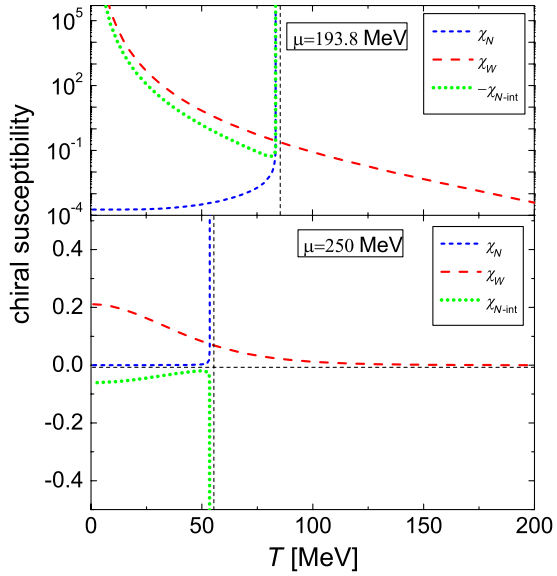

FIG. 8 (color online). Calculated temperature dependence of the chiral susceptibility at several values of chemical potential.

as chemical potential is less than 193.8 MeV. It is manifested in Fig. 8 that the susceptibility of the Nambu intermediate phase and that of the Nambu− phase are always negative if $\mu < 193.8$ MeV. It indicates that the Nambu intermediate phase and the Nambu− phase (if exists) are unstable phase(s). Meanwhile the chiral susceptibility of the Nambu+ phase is always positive before it diverges at the temperature at which the corresponding solution ϕ coalesces with that of the unstable Nambu intermediate phase. Furthermore, the susceptibility of the Wigner phase is positive at high temperature and high chemical potential and it takes negative value in the temperature region where the Nambu− phase exists. Such features of the susceptibilities of the Nambu+ phase and the Wigner phase indicate that only the Nambu+ phase (chiral symmetry broken phase) is stable in low temperature and low chemical potential region in which the susceptibility of the Nambu+ phase takes positive value and that of the Wigner phase is negative, only the Wigner phase (chiral symmetric phase) is stable in the high temperature and the high chemical potential region in which the susceptibility of the Wigner phase is positive and there does not exist Nambu solutions. Besides, there exists a region in which both the Nambu+ and the Wigner phase are stable in which both susceptibilities take positive values.

Based on the above analyses we come to the phase diagram of the system composed of three-flavor quarks in the chiral limit. The obtained result is displayed in Fig. 9, in which the upper dot-dashed line (in black) is the boundary beyond which the Nambu phase disappears, the lower dashed line (in red) is the boundary where the Wigner phase becomes (meta)stable, the region between them is that for both the Nambu phase and the Wigner phase to coexist. In the figure, the solid line (in blue) in the

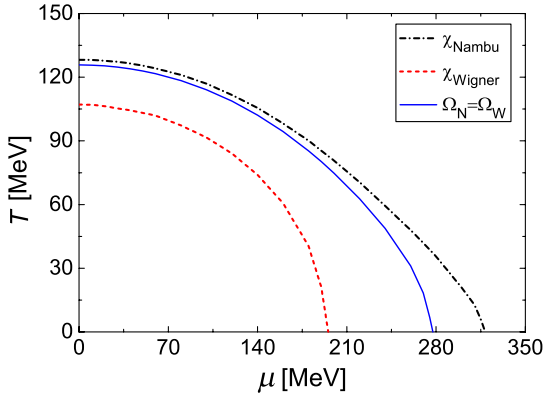

FIG. 9 (color online). Calculated phase diagram of the system consisting of three-flavor quarks in the chiral limit in temperature and chemical potential space.

middle represents the location where the thermodynamical potentials of Nambu+ and Wigner phases equate to each other. These features show apparently that the chiral susceptibility criterion to identify a chiral phase transition of the 2 + 1 flavor system is equivalent to the thermodynamical potential criterion, if the thermodynamical potential is available. Such a phase diagram shows apparently that the chiral phase transition of the system composed of three-flavor quarks in the chiral limit is in first order, which is definitely different from that of the one-flavor and two-flavor systems of which the transition is in second order or crossover [6,53]. Then there does not exist a critical end point in the phase diagram. It implies that the number of flavors affects the order of the chiral phase transition. This is in accordance with the sketch of the Colombia diagram.

B. At physical mass

We now discuss the case with physical quark masses $m_u = m_d = m_l = 5.5$ MeV, $m_s = 140.7$ MeV. The calculated results of the temperature dependence of the relative quark condensates of the light and the strange quarks [normalized by $\phi_{l0} = -(242\text{MeV})^3$, $\phi_{s0} = -(258\ \text{MeV})^3$, respectively] at zero quark chemical potential are shown in Fig. 10. The calculated flavor-mixed chiral susceptibility is shown in Fig. 11. In view of the susceptibility criterion of the chiral phase evolution, we know that the location of the peak corresponds to the pseudocritical point T_c of the chiral phase change, and it gives $T_c = 178.7$ MeV. It is apparent that such a value agrees with the lattice QCD result 175^{+1}_{-7} MeV [20] excellently and is also very close the more recent lattice QCD result $T_c \in [160, 170]$ MeV [21] for 2 + 1 flavor system. In addition, the kurtosis but nondivergent behavior of the susceptibility indicates that the chiral phase evolution is a crossover but not a second order phase transition.

The calculated results of chemical potential dependence of the normalized light quark and strange quark condensates at zero temperature are shown in Fig. 12. It is evident

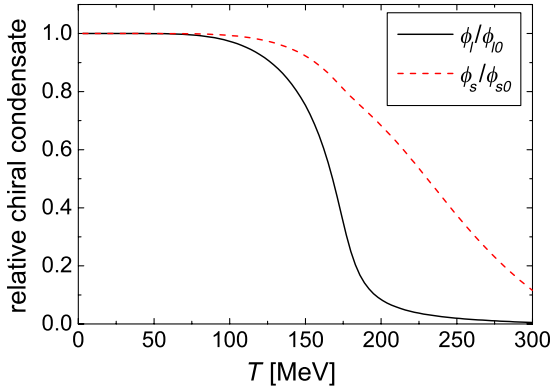

FIG. 10 (color online). Calculated temperature dependence of the relative chiral condensates at zero chemical potential of the quark with physical mass, which are normalized by ϕ_{l0} and ϕ_{s0}. The black solid line and red dashed line represent the light quark and strange quark chiral condensates, respectively.

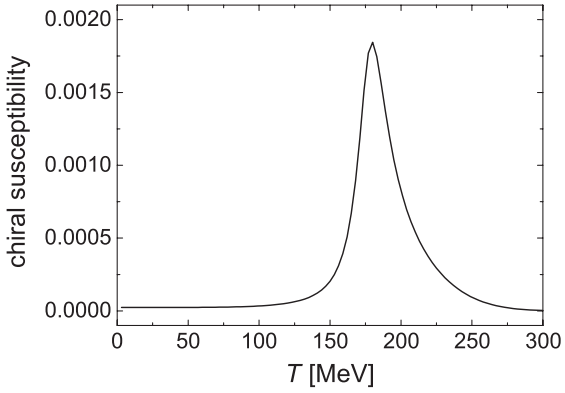

FIG. 11. Calculated temperature dependence of the chiral susceptibility of the 2 + 1 flavor quark (with physical mass) system at zero chemical potential.

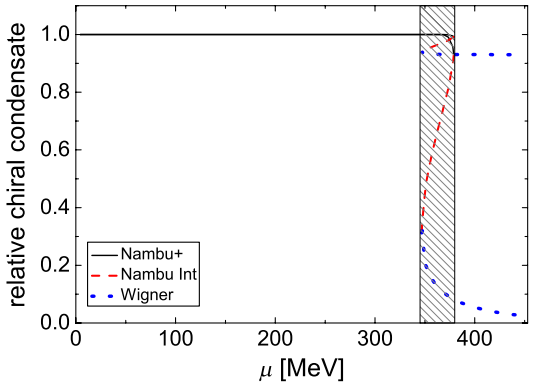

FIG. 12 (color online). Calculated chemical potential dependence of the normalized quark condensates of the 2 + 1 flavor quark (with physical mass) system at zero temperature: upper lines, strange quark condensate; lower lines, light quark condensate. The shadowed region denotes the phase of coexistence.

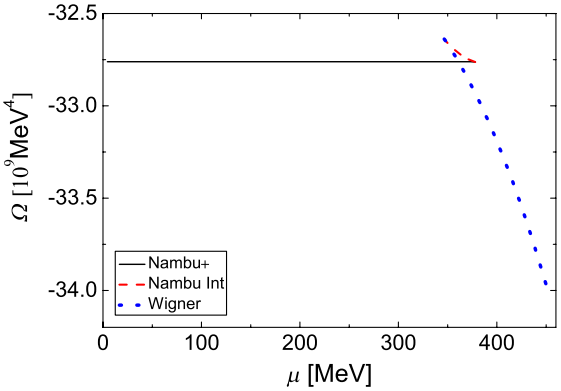

FIG. 13 (color online). Calculated chemical potential dependence of the thermodynamical potential of the $2+1$ quark (with physical mass) system at zero temperature.

that both the light quark and the strange quark condensates vary with respect to chemical potential in the same way as those in the chiral limit. The calculated variation behaviors of the effective thermodynamical potential and the flavor-mixed chiral susceptibility are illustrated in Figs. 13 and 14, respectively. The figures show apparently that there exists a chemical potential $\mu = 365.2$ MeV, below which the effective thermodynamical potential of the Nambu+ phase is the global minimum, and above which the potential of the Wigner phase becomes the global minimum. In the chemical potential region $\mu \in (348.6, 365.2)$ MeV, the potential of the Wigner phase is in the local minimum; and in the region $\mu \in (365.2, 382.1)$ MeV, the potential of the Nambu+ phase is in the local minimum. Simultaneously, as the chemical potential takes value less than 382.1 MeV, the susceptibility of the Nambu+ phase takes positive value and it diverges to positive infinity at 382.1 MeV. As the chemical potential is smaller than 348.6 MeV, the Wigner phase does not exist; thereafter, the Wigner phase appears and its chiral susceptibility takes positive value and maintains forever. It means

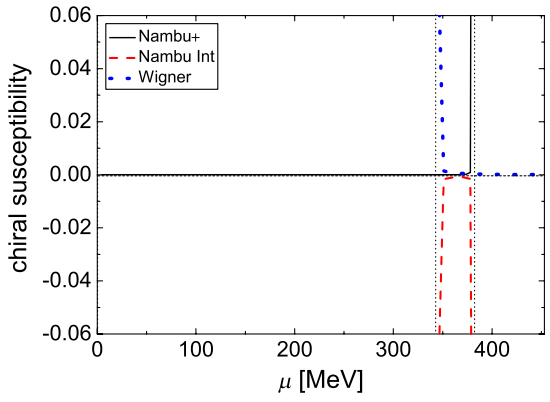

FIG. 14 (color online). Calculated chemical potential dependence of the chiral susceptibility of the $2+1$ flavor quark (with physical mass) system at zero temperature.

that there exists a chemical potential region $\mu \in [348.6, 382.1]$ MeV, in which the susceptibilities of both the Nambu+ phase and the Wigner phase are positive. These features manifest that the Nambu+ phase is stable if the chemical potential is smaller than 348.6 MeV, and the Wigner phase becomes the stable one as the chemical potential is larger than 382.1 MeV. The nature of the phase evolution driven by chemical potential is a first order phase transition. The $\mu \in [348.6, 382.1]$ MeV region is that for both the two phases to coexist. Besides, the maximum definiteness of the effective thermodynamical potential and the negative definiteness of the chiral susceptibility of the Nambu intermediate phase in the chemical potential region (348.6, 382.1) MeV indicates that the Nambu intermediate phase is always unstable. It is definite that such a characteristic of the phase transition of the $2+1$ flavor quark system is just the same as that in the chiral limit.

Taking the above discussions into account at the same time, one can get the chiral phase evolution behaviors in the two extreme cases clearly. The temperature driven phase evolution of the $2+1$ quark system at zero chemical potential is a crossover; while the chemical potential driven one (for that at zero temperature) is a first order phase transition. Thus, in the phase diagram there must exist a critical end point (CEP) at which the crossover ends and a first order phase transition region opens up. To get the complete phase diagram and fix the position of the CEP, we have performed calculations at both finite temperature and finite quark chemical potential. The obtained temperature dependence of the light quark and strange quark condensates of the $2+1$ quark system at several values of chemical potential are plotted in Fig. 15, and that of the corresponding chiral susceptibility in Fig. 16. From the figures, one can easily read that, at low chemical potential, there exists only one solution for the gap equations of the quarks, which gets smaller and smaller with the increasing of temperature. It means that the Nambu+ phase shifts, in fact, to Wigner phase continuously with the increasing of temperature. The feature of the condensates becomes more abrupt and that of the hump of chiral susceptibility gets more sharp and moves to low temperature with the increasing of chemical potential indicates that the pseudocritical temperature of the chiral phase evolution decreases with the increasing of chemical potential and the crossover gets more and more abrupt. The state for the chiral susceptibility to diverge is just that for the crossover region to disappear. Such a state is the so-called CEP state. Numerical data show that the critical end point locates at $(\mu_E, T_E) = (316.2\ \text{MeV}, 68.1\ \text{MeV})$ in the case where the masses of quarks take the corresponding physical values. As the quark chemical potential gets higher, a zigzag variation behavior appears for both the light and strange quark condensates (the same as those in Fig. 12). It means that multisolutions emerge for the condensates, and in turn, multistates coexist. Such a feature of existing

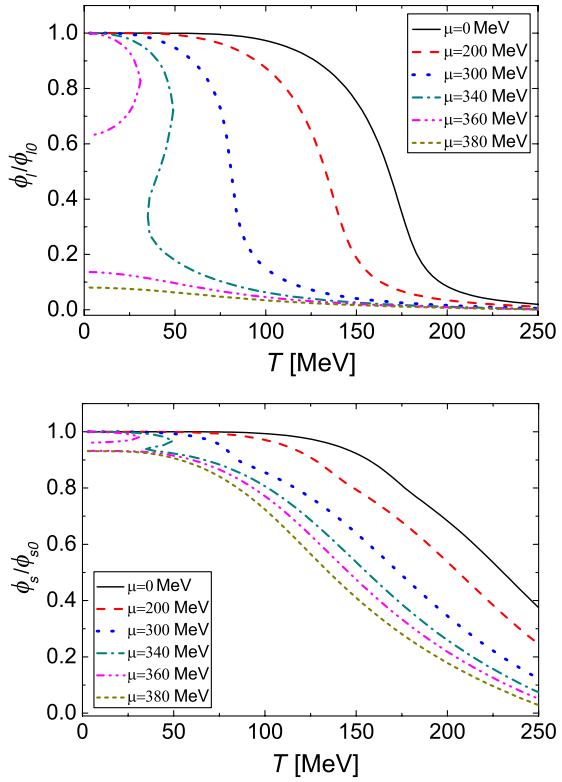

FIG. 15 (color online). Calculated temperature dependence of the normalized light quark chiral condensate at several values of the quark chemical potential (upper panel) and that of strange quark in the same condition (lower panel).

multisolutions is consistent with that for the first order transition in classical thermodynamics and also in the analytical discussion in Ref. [78]. The zigzag behavior of the condensates and the positivity of the chiral susceptibilities of both the Nambu+ phase and the Wigner phase thereafter indicate then that the phase evolution changes from crossover to first order phase transition definitely in the intermediate chemical potential region.

As the chemical potential grows much higher, the Nambu phase disappears, but only the Wigner phase with positive chiral susceptibility exists. It means that the chiral symmetry has restored.

With the above results in mind, we can reach the phase diagram of the 2 + 1 flavor quark system with physical masses. The obtained result is illustrated as the blue lines in Fig. 17. We now have had not only the phase boundaries but also the position of the CEP. As mentioned above, at physical masses, the CEP locates at $(\mu_E, T_E) = (316.2\ \text{MeV}, 68.1\ \text{MeV})$. It is apparent that the value $\mu_E/T_E = 4.643$ is quite close to the results given by other NJL model and PNJL(-like) calculations (see for example Refs. [47,58–61]) but larger than that given in the Dyson-Schwinger equation calculation [34,37,38] and those in lattice QCD simulations [13–16]. As pointed out in Ref. [37], such an inconsistency comes from the fact that the confinement length in the NJL model is zero.

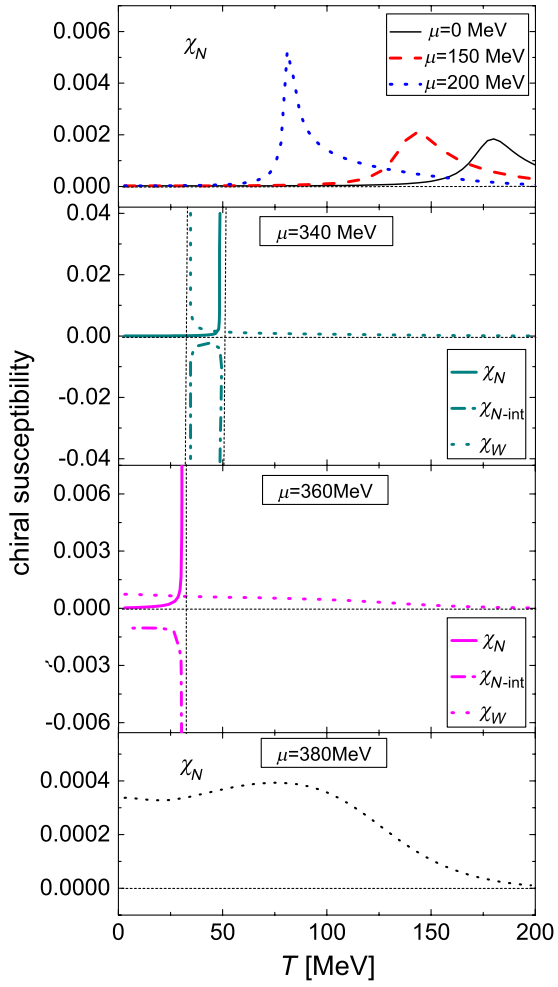

FIG. 16 (color online). Calculated temperature dependence of the chiral susceptibilities of the 2 + 1 flavor quark system with physical mass at several values of chemical potential.

Comparing the appearance of the phase diagrams obtained with different criteria, one can notice again that the chiral susceptibility criterion for identifying a chiral phase transition of the 2 + 1 flavor system is equivalent to the thermodynamical potential criterion.

C. Phase diagram in 3D space

It has been known that the QCD phase diagram depends on many aspects, such as the intrinsic parameters of current quark masses and interaction strengths (see, for example, Ref. [32]), the medium effects of temperature and chemical potential. Then the complete QCD phase diagram should be multidimensional. To be concise and simple, we consider in this paper the three-dimensional (3D) one in terms of temperature, quark chemical potential, and strange quark mass with the above fixed interaction strength parameters and that in terms of the temperature, quark chemical potential and the $U_A(1)$ anomaly strength (the six-point flavor-mixing interaction strength) K (or $K\Lambda^5$) with the physical quark masses.

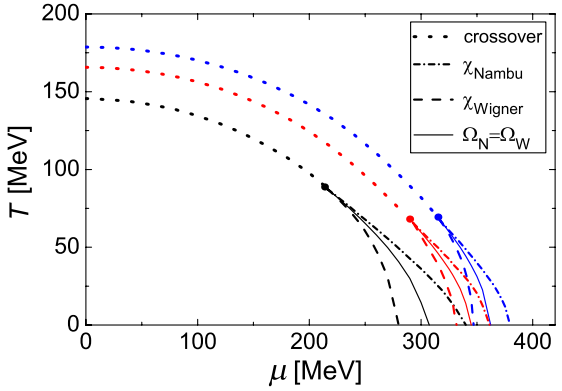

FIG. 17 (color online). Calculated phase diagrams in terms of temperature and chemical potential at different values of current strange quark mass. The right (in blue) is at physical masses, the middle (in red) is at $m_s = 50$ MeV, $m_l = 5.5$ MeV, and the left (in black) is at $m_s = m_l = 5.5$ MeV. In each case, the dotted line stands for the set of states for the chiral susceptibility to take the value at the top of hump, the dashed line is that of the states for the chiral susceptibility of the Wigner phase to diverge and become positive, the dot-dashed line represents the states for the chiral susceptibility of the Nambu phase to diverge and then disappear, and the filled circle labels the CEP. The dotted line together with the solid line is the phase boundary determined with the usual thermodynamical potential criterion.

After plenty of calculations, we get the phase diagrams in the above-mentioned two cases. The obtained phase diagram in the space of temperature, chemical potential, and strange quark mass is illustrated in Fig. 18. The states

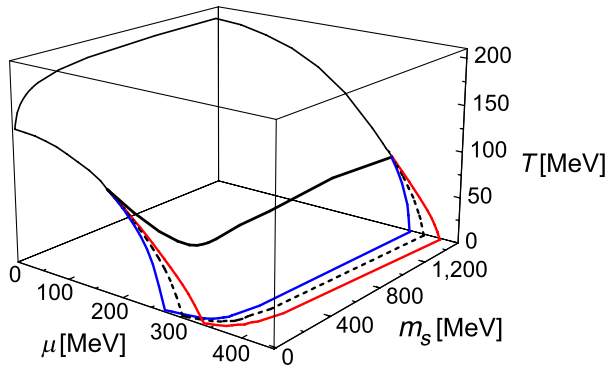

FIG. 18 (color online). Calculated three-dimensional phase diagram in terms of the strange quark mass, chemical potential, and temperature (in m_s-μ-T space) of the $2 + 1$ flavor quark system. The thin solid black lines stand for the set of states for the chiral susceptibility to take the value at the top of hump, the solid blue lines are the set of states for the chiral susceptibility of the Wigner phase to diverge and become positive, and the solid red lines represent the states for the chiral susceptibility of the Nambu phase to diverge and then disappear. The thick solid line in black is the set of CEPs and the region between the red and blue lines is the coexistence region. The thin solid black line together with the dotted black line is the phase boundary determined with the usual thermodynamical potential criterion.

on the curved surface with boundary in the solid black lines are the pseudocritical states of the crossover of chiral phase evolution. The region between the camber with boundary in the solid red lines and that in the blue lines is that for the chiral symmetry broken and chiral symmetric phases to coexist. The thick solid curve (in black) is just that representing the CEPs. Its variation behavior can be approximately written in a set of parametrized equations in terms of the current strange quark mass as

$$\frac{\mu_E}{\mu_0} = 1 - \frac{c_1}{\frac{m_s}{m_l} + r_0}, \tag{13}$$

with $\mu_0 = 331.7$ MeV, $r_0 = 3.032$, and $c_1 = 1.452$;

$$\frac{T_E}{T_0} = 1 - \frac{c_1'}{\frac{m_s}{m_l} + r_0'} + \frac{c_2'}{(\frac{m_s}{m_l} + r_0')^2}, \tag{14}$$

with $T_0 = 87.8$ MeV, $r_0' = 9.686$, $c_1' = 11.39$, and $c_2' = 125.8$.

From the diagram, we can notice that the region of the coexistence opens up from a critical end point and grows wider with the decrease of m_s. However, the chiral phase evolution is still a crossover at the low chemical potential region even if the current strange quark mass goes down to zero. To manifest such a feature more clearly, we display the phase diagram (or that of the projection) in the T-μ plane in case of $m_s = 50$ MeV and $m_l = 5.5$ MeV and that with $m_s = m_l = 5.5$ MeV in Fig. 17. The figure also indicates that the location of the CEP depends on the temperature, the chemical potential, and the strange quark mass. For instance, as the strange quark mass changes from 50 MeV to 5.5 MeV, the location of the CEP moves from $(\mu_E, T_E) = (292.8\ \text{MeV}, 65.7\ \text{MeV})$ to (215.8 MeV, 87.7 MeV).

To demonstrate the variation feature of the CEP more intuitively, we show the projection of CEP's track on the m_s-μ plane and that on the m_s-T plane in Fig. 19. It is apparent that the quark chemical potential of the CEP shows a generally upward tendency as the strange quark mass increases in the region with small values and gets almost saturated as the mass grows quite large. For instance, it runs from 171.6 MeV at $m_s = 0$ MeV to 316.2 MeV at $m_s = 140.7$ MeV, then to 328.5 MeV at $m_s = 500.0$ MeV, and further 331.7 MeV at very large strange quark mass. While, contrary to the variation characteristic of the chemical potential, the temperature of the CEP behaves at a downward tendency as the strange quark mass increases in the region with small values and turns to be larger as the mass becomes very large. From the figure and Eq. (14), one can read that the temperature of the CEP, T_E, changes from 103.9 MeV at $m_s = 0$ MeV to 68.1 MeV at $m_s = 140.7$ MeV, and 77.3 MeV at $m_s = 500.0$ MeV, then saturates at 87.9 MeV if the strange quark mass is extremely large. These features indicate that for the quark system with two light flavors and one very heavy flavor, the CEP locates at $(\mu_E^S, T_E^S) = (331.7\ \text{MeV}, 87.9\ \text{MeV})$. Such

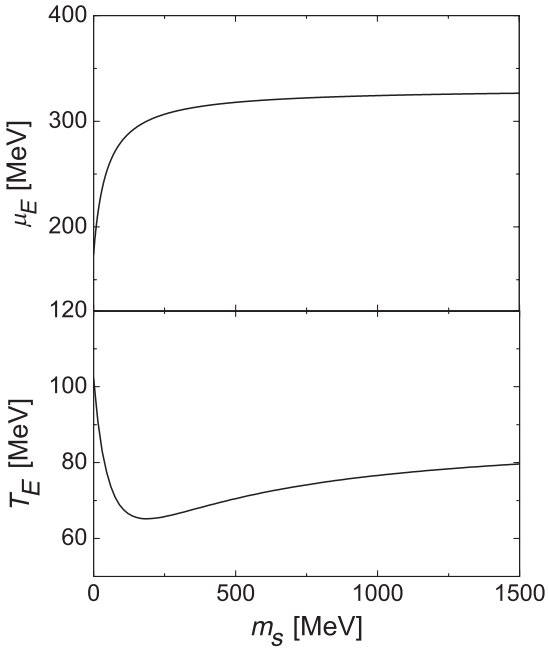

FIG. 19. Calculated projection of the CEP's track on the m_s-μ plane (upper panel) and on the m_s-T plane (lower panel).

a characteristic of the CEP's variation with respect to the strange quark mass is qualitatively similar to that given in Refs. [47,59] with other criterion.

The obtained phase diagram in terms of the $U_A(1)$ anomaly strength, the temperature, and the chemical potential (in the K-μ-T space) is shown in Fig. 20. Similar to that in Fig. 18, the region in which the chiral phase evolution is in crossover is also demonstrated by a curved surface with boundaries in solid black lines and the thick part displays the track of the CEPs, and the region for the chiral phase evolution to be a first order phase transition by that with solid red lines and blue lines (the region between the red and the blue lines is the coexistence region). The track of the CEPs within the region of our concern can be approximately written in a set of parametrized equations in terms of the parameter $K\Lambda^5$ as

$$\frac{\mu_E}{\Lambda} = c_0 + c_1(K\Lambda^5) + c_2(K\Lambda^5)^2, \tag{15}$$

with $c_0 = 0.4263$, $c_1 = 0.01493$, and $c_2 = -0.0005629$;

$$\frac{T_E}{\Lambda} = [c_0' + c_1'(K\Lambda^5) + c_2'(K\Lambda^5)^2]^{1/2}, \tag{16}$$

with $c_0' = -0.005998$, $c_1' = 0.0005028$, and $c_2' = 0.00008078$.

To show the effect of the $U_A(1)$ anomaly on the phase diagram more clearly, we demonstrate the projection of the CEPs on the μ-K plane and the T-K plane in Fig. 21 and replot the phase diagram of the system with physical masses in terms of temperature and chemical potential at three different values of the K in Fig. 22, where the line in the left (in blue) is the result at $K\Lambda^5 = 0$, the middle (in red) is that at $K\Lambda^5 = 12.36$, and the right (in black) illustrates that at $K\Lambda^5 = 28$. It is apparent that, different from the effect of current strange quark mass (shown in Fig. 18), weak $U_A(1)$ anomaly does not induce the property of the chiral phase evolution from a crossover to a first order phase transition. The critical strength for the phase evolution behavior to change is $K\Lambda^5 \approx 6.05$. When the $U_A(1)$ anomaly strength reaches the critical value $(K\Lambda^5)_c \approx 6.05$, a first order phase transition appears and a critical end point emerges. With the increasing of the value of K, the region of the first order phase transition gets wider and wider and the temperature of the CEP raises obviously. Looking over Figs. 21 and 22

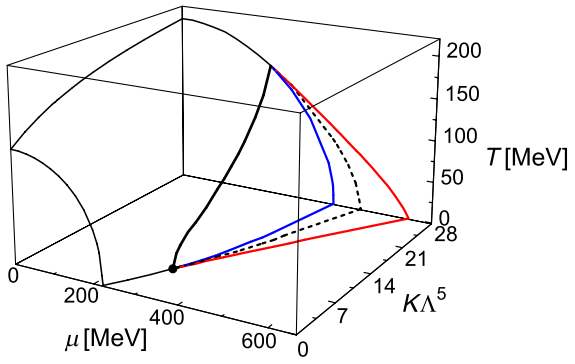

FIG. 20 (color online). Calculated three-dimensional phase diagram in terms of the $U_A(1)$ anomaly (six-point flavor-mixing interaction, or the triple chiral coupling) strength, temperature, and chemical potential (in K-T-μ space) of the $2+1$ flavor quark system with physical masses. The symbols of the lines are the same as those in Fig. 18 correspondingly.

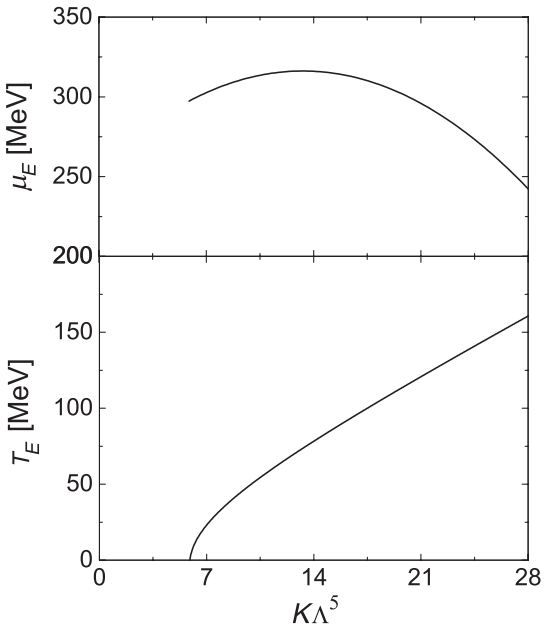

FIG. 21. Calculated projection of the CEP's track on the K-μ plane (upper panel) and on the K-T plane (lower panel).

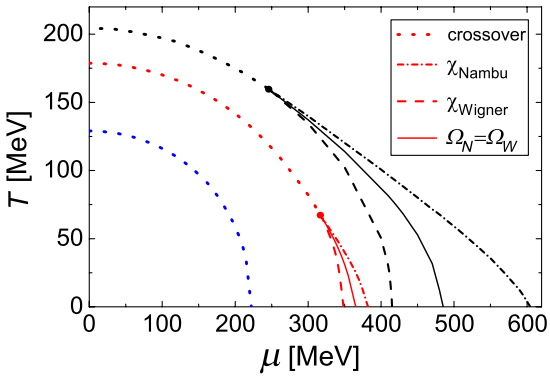

FIG. 22 (color online). Calculated phase diagrams in terms of temperature and chemical potential at different values of the $U_A(1)$ anomaly (six-point interaction) strength with $m_l = 5.5$ MeV, $m_s = 140.7$ MeV. The left (in blue) is at $K\Lambda^5 = 0$, the middle (in red) is at $K\Lambda^5 = 12.36$, and the right (in black) is at $K\Lambda^5 = 28$. The symbol of each line is the same as the corresponding one in Fig. 17.

more carefully, one can observe that, with the increasing of the $U_A(1)$ anomaly strength, the temperature of the CEP increases monotonically, but the chemical potential increases first and then becomes smaller. For instance, as the strength $K\Lambda^5$ increases from 6.05 to 12.36 and then to 28, the critical end point runs from $(K\Lambda^5, \mu_E, T_E) = (6.05, 297.9\ \text{MeV}, 0\ \text{MeV})$ to $(12.36, 316.2\ \text{MeV}, 68.1\ \text{MeV})$ and further $(28, 243.6\ \text{MeV}, 160.4\ \text{MeV})$. It indicates that the triple chiral coupling K, a part of the $U_A(1)$ anomaly, favors the first order phase transition and pushes the CEP away from the chemical potential axes. Such a feature of the effect of the triple chiral coupling which induces the flavor mixing is obviously consistent with the previous results [47,59,72]. However, the exact phase structure might, in fact, be much more complicated at high chemical potential and low temperature, since the six-point interaction we take into account in the present paper is only one type of the $U_A(1)$ anomaly, which describes the triple chiral coupling. As the other type of the $U_A(1)$ anomaly, which demonstrates the chiral diquark coupling, is taken into account simultaneously, previous investigations [70–72] show that the first order phase transition in the high chemical potential region turns into a BEC-BCS crossover and leads a new CEP to appear.

IV. SUMMARY AND REMARK

In summary, we have restudied the chiral phase transition of the 2 + 1 flavor quark system in the NJL model, with emphasis on the current quark mass and the flavor-mixing triple chiral coupling [a type of $U_A(1)$ anomaly] effects on the phase diagram and, especially the location of the critical end point. We extended the recently proposed chiral susceptibility criterion to determine the phase boundary and the location of the CEP for the one-flavor (or two symmetric flavor) quark system to three-flavor system. With the new criterion, we gave the phase diagram of the 2 + 1 quark system in terms of the temperature, quark chemical potential and strange quark mass and that in terms of the temperature, quark chemical potential and flavor-mixing triple chiral coupling strength. We located the CEP of the 2 + 1 quark system with physical masses at $(\mu_E, T_E) = (316.2\ \text{MeV}, 68.1\ \text{MeV})$ (or with ratio $\mu_E/T_E = 4.643$) which is quite close to the previous results given in the NJL model and PNJL(-like) calculations. We also show that the more massive the strange quark much lower the temperature and much higher the chemical potential of the CEP if the mass is not quite large. For the effect of the flavor-mixing interaction strength, there exists a critical value $(K\Lambda^5)_c \approx 6.05$ for the crossover to turn into a first order phase transition. Increasing the flavor-mixing strength beyond the critical one induces the temperature of the CEP to increase drastically and enhances the chemical potential slightly if the strength is not very large. These variation features are also consistent with previous results. Such an investigation provides, on one hand, further evidence that the chiral susceptibility criterion is quite efficient in not only determining the phase boundary but also fixing the position of the CEP. On the other hand, it indicates that the CEP of QCD phase transition depends definitely not only on the temperature and density (chemical potential) of the system but also on the intrinsic parameters such as the current quark mass and the interaction strengths. On the theory side, even though plenty of calculations have been carried out (besides those mentioned above, see also, for example, Refs. [79–81]) and the newly proposed chiral susceptibility criterion is quite practical, really manageable methods on the location of the CEP of QCD need still efforts to develop. On the experiment side, one hopes that the low energy scan of RHIC at BNL and the future FAIR experiment at GSI (see, for instance, Refs. [82,83]) may shed light on that. Concerning our present results, we would propose that the signals of the CEP related to very heavy flavor quark may be paid much attention since its position is well fixed.

In addition, it is well known that the NJL model does not take the confinement effect into account and considering the Polyakov loop effect is practical to include the contribution of the confinement. It has also been known that the vector component of the interaction plays an important role in the fluctuation behavior of the conserved charges [84] and the structure of the QCD vacuum [85]. Furthermore, to study the 2 + 1 flavor quark system practically, one needs to consider the isospin chemical potential of light quarks or the different chemical potential of strange quarks. The relevant works are under progress. However, as a first step to investigate both the quark mass and flavor-mixing effects with a new criterion to identify the phase evolution and the CEP, we have not yet taken these aspects into account in this paper.

ACKNOWLEDGMENTS

The work was supported by National Natural Science Foundation of China under Contracts No. 10935001, No. 11075052, and No. 11175004, and the National Key Basic Research Program of China under Contract No. G2013CB834400. S.-x. Q. thanks also the support of Alexander von Humboldt Foundation via a Research Fellowship for Postdoctorial Researchers.

[1] N. Itoh, Prog. Theor. Phys. **44**, 291 (1970); D. A. Kirzhnits and A. D. Linde, Phys. Lett. **42B**, 471 (1972).
[2] T. D. Lee and G. C. Wick, Phys. Rev. D **9**, 2291 (1974).
[3] J. C. Collins and M. J. Perry, Phys. Rev. Lett. **34**, 1353 (1975).
[4] B. Svetitsky, Phys. Rep. **132**, 1 (1986).
[5] H. Meyer-Ortmanns, Rev. Mod. Phys. **68**, 473 (1996).
[6] D. H. Rischke, Prog. Part. Nucl. Phys. **52**, 197 (2004).
[7] F. Wilczek, Nature (London) **443**, 637 (2006); arXiv:0809.3137.
[8] P. Braun-Munzinger and J. Wambach, Rev. Mod. Phys. **81**, 1031 (2009).
[9] K. Fukushima and T. Hatsuda, Rep. Prog. Phys. **74**, 014001 (2011); K. Fukushima, J. Phys. G **39**, 013101 (2012).
[10] F. Karsch, Lect. Notes Phys. **583**, 209 (2002).
[11] J. Greensite, Prog. Part. Nucl. Phys. **51**, 1 (2003).
[12] P. Petreczky, J. Phys. G **39**, 093002 (2012).
[13] Z. Fodor and S. D. Satz, Phys. Lett. B **534**, 87 (2002); J. High Energy Phys. 03 (2002) 014; 04 (2004) 050; R. V. Gavai and S. Gupta, Phys. Rev. D **71**, 114014 (2005); S. Gupta, Proc. Sci., CPOD2009 (2009) 025.
[14] P. de Forcrand and S. Kratochvila, Nucl. Phys. B, Proc. Suppl. **153**, 62 (2006).
[15] S. Ejiri, Phys. Rev. D **77**, 014508 (2008).
[16] A. Y. Li, A. Alexandru, X. F. Meng, and K. F. Liu, Nucl. Phys. **A830**, 633c (2009); A. Y. Li, A. Alexandru, and K. F. Liu, Phys. Rev. D **84**, 071503 (2011).
[17] P. de Forcrand and O. Philipsen, Phys. Rev. Lett. **105**, 152001 (2010).
[18] T. Misumi, T. Kimura, and A. Ohnishi, Phys. Rev. D **86**, 094505 (2012).
[19] Y. Aoki, G. Endrodi, Z. Fodor, S. D. Katz, and K. K. Szabo, Nature (London) **443**, 675 (2006).
[20] S. Gupta, X. F. Luo, B. Mohanth, H. G. Ritter, and N. Xu, Science **332**, 1525 (2011).
[21] A. Bazavov *et al.* (HotQCD Collaboration), Phys. Rev. D **86**, 034509 (2012).
[22] M. Hanada, Y. Matsuo, and N. Yamamoto, Phys. Rev. D **86**, 074510 (2012); K. Nagata, S. Motoki, Y. Nakagawa, A. Nakamura, and T. Saito, Prog. Theor. Exp. Phys. **2012**, 01A103 (2012); S. Ejiri, K. Kanaya, and T. Umeda, Prog. Theor. Exp. Phys. **2012**, 01A104 (2012); D. Grabowska, D. B. Kaplan, and A. N. Nicholson, Phys. Rev. D **87**, 014504 (2013).
[23] S. Chandrasekharan and A. Li, Phys. Rev. Lett. **108**, 140404 (2012); Phys. Rev. D **85**, 091502(R) (2012).
[24] C. D. Roberts and A. G. Williams, Prog. Part. Nucl. Phys. **33**, 477 (1994); C. D. Roberts and S. M. Schmidt, Prog. Part. Nucl. Phys. **45**, S1 (2000); C. D. Roberts, M. S. Bhagwat, A. Höll, and S. V. Wright, Eur. Phys. J. Special Topics **140**, 53 (2007); C. D. Roberts, arXiv:1203.5341.
[25] R. Alkofer and L. von Smekal, Phys. Rep. **353**, 281 (2001).
[26] P. Maris and C. D. Roberts, Int. J. Mod. Phys. E **12**, 297 (2003).
[27] C. S. Fischer, J. Phys. G **32**, R253 (2006).
[28] A. Bashir, L. Chang, I. C. Cloet, B. El-Bennich, Y. X. Liu, C. D. Roberts, and P. C. Tandy, Commun. Theor. Phys. **58**, 79 (2012).
[29] C. D. Roberts and B. H. J. McKellar, Phys. Rev. D **41**, 672 (1990).
[30] L. Chang, Y. X. Liu, M. S. Bhagwat, C. D. Roberts, and S. V. Wright, Phys. Rev. C **75**, 015201 (2007); L. Chang, B. Wang, W. Yuan, H. Chen, G. Y. Shao, and Y. X. Liu, Int. J. Mod. Phys. E **16**, 2289 (2007); Y. Jiang, H. Gong, W. M. Sun, and H. S. Zong, Phys. Rev. D **85**, 034031 (2012).
[31] R. Williams, C. S. Fischer, and M. R. Pennington, Phys. Lett. B **645**, 167 (2007); C. S. Fischer, D. Nickel, and R. Williams, Eur. Phys. J. C **60**, 47 (2009).
[32] K. L. Wang, S. X. Qin, Y. X. Liu, L. Chang, C. D. Roberts, and S. M. Schmidt, Phys. Rev. D **86**, 114001 (2012).
[33] D. Blaschke, C. D. Roberts, and S. M. Schmidt, Phys. Lett. B **425**, 232 (1998).
[34] M. He, J. F. Li, W. M. Sun, and H. S. Zong, Phys. Rev. D **79**, 036001 (2009).
[35] W. Yuan, H. Chen, and Y. X. Liu, Phys. Lett. B **637**, 69 (2006).
[36] L. Chang, H. Chen, B. Wang, W. Yuan, and Y. X. Liu, Phys. Lett. B **644**, 315 (2007); H. Chen, W. Yuan, L. Chang, Y. X. Liu, T. Klähn, and C. D. Roberts, Phys. Rev. D **78**, 116015 (2008); M. He, D. K. He, H. T. Feng, W. M. Sun, and H. S. Zong, Phys. Rev. D **76**, 076005 (2007); H. S. Zong and W. M. Sun, Phys. Rev. D **78**, 054001 (2008); Y. Jiang, L. J. Luo, and H. S. Zong, J. High Energy Phys. 02 (2011) 066.
[37] S. X. Qin, L. Chang, H. Chen, Y. X. Liu, and C. D. Roberts, Phys. Rev. Lett. **106**, 172301 (2011).
[38] C. S. Fischer, J. Luecker, and J. A. Mueller, Phys. Lett. B **702**, 438 (2011); C. S. Fischer and J. Luecker, Phys. Lett. B **718**, 1036 (2013).
[39] D. Nickel, Ann. Phys. (Amsterdam) **322**, 1949 (2007); J. A. Mueller, C. S. Fischer, and D. Nickel, Eur. Phys. J. C **70**, 1037 (2010); S. X. Qin, L. Chang, Y. X. Liu, and C. D. Roberts, Phys. Rev. D **84**, 014017 (2011).
[40] D. Nickel, J. Wambach, and R. Alkofer, Phys. Rev. D **73**, 114028 (2006); D. Nickel, R. Alkofer, and J. Wambach, Phys. Rev. D **74**, 114015 (2006); F. Marhauser, D. Nickel, M. Buballa, and J. Wambach, Phys. Rev. D **75**, 054022

(2007); D. Nickel, R. Alkofer, and J. Wambach, Phys. Rev. D **77**, 114010 (2008).
[41] Y. Nambu and G. Jona-Lasinio, Phys. Rev. **122**, 345 (1961); **124**, 246 (1961).
[42] U. Vogl and W. Weise, Prog. Part. Nucl. Phys. **27**, 195 (1991); S. P. Klevansky, Rev. Mod. Phys. **64**, 649 (1992); T. Hatsuda and T. Kunihiro, Phys. Rep. **247**, 221 (1994); R. Alkofer, H. Reinhardt, and H. Weigel, Phys. Rep. **265**, 139 (1996); M. Buballa, Phys. Rep. **407**, 205 (2005).
[43] C. Hattori, M. Kobayash, H. Kondo, and T. Maskawa, Prog. Theor. Phys. **43**, 1334 (1970); M. Kobayash, H. Kondo, and T. Maskawa, Prog. Theor. Phys. **45**, 1955 (1971); H. Pagels, Phys. Rev. Lett. **28**, 1482 (1972).
[44] A. Manohar and H. Georgi, Nucl. Phys. **B234**, 189 (1984).
[45] P. Guichon, Phys. Lett. B **200**, 235 (1988); K. Saito, K. Tsushima, and A. W. Thomas, Prog. Part. Nucl. Phys. **58**, 1 (2007).
[46] K. Fukushima, Phys. Lett. B **591**, 277 (2004); C. Ratti, M. A. Thaler, and W. Weise, Phys. Rev. D **73**, 014019 (2006).
[47] W. J. Fu, Z. Zhang, and Y. X. Liu, Phys. Rev. D **77**, 014006 (2008).
[48] M. Ciminale, R. Gatto, N. D. Ippolito, G. Nardulli, and M. Ruggieri, Phys. Rev. D **77**, 054023 (2008).
[49] B.-J. Schaefer, J. M. Pawlowski, and J. Wambach, Phys. Rev. D **76**, 074023 (2007); T. K. Herbst, J. M. Pawlowski, and B.-J. Schaefer, Phys. Lett. B **696**, 58 (2011); B.-J. Schaefer and M. Wagner, Phys. Rev. D **85**, 034027 (2012).
[50] S. Chatterjee and K. A. Mohan, Phys. Rev. D **85**, 074018 (2012).
[51] B. J. Schaefer and J. Wambach, Prog. Part. Nucl. Phys. **39**, 1025 (2008); B.-J. Schaefer and M. Wagner, Prog. Part. Nucl. Phys. **62**, 381 (2009).
[52] U. S. Gupta and V. K. Tiwari, Phys. Rev. D **85**, 014010 (2012); V. K. Tiwari, Phys. Rev. D **86**, 094032 (2012).
[53] A. J. Peterson, Nucl. Phys. **B190**, 188 (1981); R. D. Pisarski and D. J. Stein, J. Phys. A **14**, 3341 (1981); R. D. Pisarski and F. Wilczek, Phys. Rev. D **29**, 338 (1984).
[54] W. Cassing and E. L. Bratkovskaya, Phys. Rep. **308**, 65 (1999).
[55] Y. Hatta and T. Ikeda, Phys. Rev. D **67**, 014028 (2003).
[56] P. Kovács and Zs. Szép, Phys. Rev. D **77**, 065016 (2008).
[57] V. Skokov, B. Stokic, B. Friman, and K. Redlich, Phys. Rev. C **82**, 015206 (2010).
[58] C. Sasaki, B. Friman, and K. Redlich, Phys. Rev. D **77**, 034024 (2008); P. Costa, M. C. Ruivo, and C. A. de Sousa, Phys. Rev. D **77**, 096001 (2008).
[59] K. Fukushima, Phys. Rev. D **77**, 114028 (2008).
[60] K. Kashiwa, H. Kouno, M. Matsuzaki, and M. Yahiro, Phys. Lett. B **662**, 26 (2008); H. Abuki, R. Anglani, R. Gatto, G. Nardulli, and M. Ruggieri, Phys. Rev. D **78**, 034034 (2008); B.-J. Schaefer and M. Wagner, Phys. Rev. D **79**, 014018 (2009); P. Costa, H. Hansen, M. C. Ruivo, and C. A. de Sousa, Phys. Rev. D **81**, 016007 (2010).
[61] T. Sasaki, Y. Sakai, H. Kouno, and M. Yahiro, Phys. Rev. D **84**, 091901(R) (2011).
[62] E. S. Bowman and J. I. Kapusta, Phys. Rev. C **79**, 015202 (2009).
[63] H. Mao, J. S. Jin, and M. Huang, J. Phys. G **37**, 035001 (2010).
[64] F. K. Xu, H. Mao, T. K. Mukherjee, and M. Huang, Phys. Rev. D **84**, 074009 (2011).
[65] P. K. Srivastava, S. K. Tiwari, and C. P. Singh, Phys. Rev. D **82**, 014023 (2010).
[66] V. Skokov, B. Friman, and K. Redlich, Phys. Rev. C **83**, 054904 (2011).
[67] O. Kaczmarek, F. Karsch, E. Laermann, C. Miao, S. Mukherjee, P. Petreczky, C. Schmidt, W. Soeldner, and W. Unger, Phys. Rev. D **83**, 014504 (2011).
[68] K. Fukushima, Phys. Rev. D **86**, 054002 (2012).
[69] T. Inagaki, D. Kimura, H. Kohyaka, and A. Kvinikhidze, arXiv:1202.5220.
[70] T. Hatsuda, M. Tachibana, N. Yamamoto, and G. Baym, Phys. Rev. Lett. **97**, 122001 (2006).
[71] G. Baym, T. Hatsuda, M. Tachibana, and N. Yamamoto, J. Phys. G **35**, 104021 (2008).
[72] H. Abuki, G. Baym, T. Hatsuda, and N. Yamamoto, Phys. Rev. D **81**, 125010 (2010).
[73] P. D. Powell and G. Baym, Phys. Rev. D **85**, 074003 (2012).
[74] O. Philipsen, Acta Phys. Pol. B Proc. Suppl. **5**, 825 (2012).
[75] Y. Hidaka and N. Yamamoto, J. Phys. Conf. Ser. **432**, 012017 (2013).
[76] Y. Zhao, L. Chang, W. Yuan, and Y. X. Liu, Eur. Phys. J. C **56**, 483 (2008).
[77] P. Rehberg, S. P. Klevansky, and J. Hüfner, Phys. Rev. C **53**, 410 (1996).
[78] B. Friman, Acta Phys. Pol. B **5**, 707 (2012).
[79] M. A. Stephanov, K. Rajagopal, and E. V. Shuryak, Phys. Rev. Lett. **81**, 4816 (1998); M. A. Stephanov, Prog. Theor. Phys. Suppl. **153**, 139 (2004); Phys. Rev. Lett. **107**, 052301 (2011); J. Phys. G **38**, 124147 (2011).
[80] M. Ruggieri, Phys. Rev. D **84**, 014011 (2011).
[81] J. Xiong, M. Jin, and J. R. Li, Phys. Rev. C **83**, 025204 (2011).
[82] C. Blume, Central Eur. J. Phys. **10**, 1245 (2012); S. A. Bass, H. Petersen, C. Quammen, H. Canary, C. G. Healey, and R. M. Taylor II, Cent. Eur. J. Phys. **10**, 1278 (2012).
[83] J. Eschke, Eur. Phys. J. Web Conf. **20**, 05002 (2012).
[84] T. Kunihiro, Phys. Lett. B **271**, 395 (1991).
[85] M. N. Chernodub, Phys. Rev. D **82**, 085011 (2010); Phys. Rev. Lett. **106**, 142003 (2011).